Coordinating the Interplay between Physical Carrier Sense and Power Control in CSMA/CA Wireless Networks

Kyung-Joon Park, LaeYoung Kim, and Jennifer C. Hou
Department of Computer Science
University of Illinois at Urbana-Champaign
Urbana, IL 61801 USA
Email: {kjp, laeyoung, jhou}@uiuc.edu

***Abstract*—The transmit power and the carrier sense threshold are two major MAC/PHY parameters in CSMA/CA wireless networks. The problem of transmit power control has been extensively studied in the context of graph-theoretic topology control and maintenance. What has not been studied in depth is the effect of signal to interference plus noise ratio (SINR) on the topology and the network capacity sustained under the physical model. In order to remedy the deficiency of conventional topology control (as a result of neglecting the physical SINR effect) and to further improve network performance, we present a joint control framework for determining the transmit power control and the carrier sense threshold. We identify that the joint control problem can be decoupled into two sub-problems: conventional topology control and dynamic control of carrier sense threshold. We then derive a desirable operating condition for the carrier sense threshold. We show that there exists an abrupt increase in the collision probability as the carrier sense threshold increases, and that this transition can be efficiently identified by observing the collision probability. Thus, to maximize the node throughput, each node may increase the carrier sense threshold as long as the collision probability is below a reasonable threshold.**

Based on the insight shed from our analysis, we devise a dynamic tuning algorithm for carrier sense thresholds, by which each node observes its local event (i.e., transmission collisions) and drives its carrier sense threshold towards the desirable operating point in a fully distributed manner. To demonstrate the utility of the proposed joint control framework, we equip a localized topology control algorithm, localized minimal spanning tree (LMST), with the capability of dynamic carrier sense adaptation (DCSA). Via simulation, we show that *joint control* of transmit power and carrier sense threshold is crucial for improving the network performance and that the resulting control algorithm LMST-DCSA significantly outperforms LMST alone.

***Index Terms*—CSMA/CA wireless network; physical carrier sense; topology control; MAC throughput.**

I. Introduction

Multi-hop wireless networks, e.g., wireless mesh networks, have emerged to be a promising, cost-effective technology for next-generation wireless networking [1]. Their major advantage is the capability of building networks without a pre-installed central infrastructure. In particular, in CSMA/CA multi-hop wireless networks, instead of using a central entity for coordinating the radio channel, a distributed access mechanism is deployed at each node to arbitrate channel access.

Several PHY/MAC attributes in CSMA/CA networks can be used to arbitrate channel access, to mitigate interference, and to improve network capacity, among which we focus on the *transmit power* and the *carrier sense threshold*. This is because the network capacity, i.e., the average data bits that can be transported simultaneously in the network, heavily depends on the level of spatial reuse characterized by physical carrier sense. Under physical carrier sense, a sender senses the channel before each transmission and determines whether or not the channel is busy by comparing the received signal strength with the carrier sense threshold. If the signal strength is below the carrier sense threshold, the sender considers the channel to be idle and starts its transmission. Otherwise, the sender considers the channel to be busy and enters in the collision avoidance phase. Since the received signal strength is, in principle, proportional to the transmit power of the sender, both the carrier sense threshold and the transmit power are major control knobs for exploiting spatial reuse.

In this paper, we consider the problem of how to design an efficient algorithm for jointly controlling the transmit power and the carrier sense threshold. Although abundant research results already exist in the context of graph-theoretic topology control [2]–[6], most of them have neglected the effect of the signal to interference plus noise ratio (SINR), which is critical for successful transmission under the physical model. Moscibroda *et al.* [7] are perhaps the first to consider topology control under the physical SINR model and investigated the time complexity of centralized scheduling for topology-controlled networks. Complementing their work, we consider the problem in a more practical setting, i.e., CSMA/CA wireless networks. We aim to answer the following fundamental questions — can one leverage existing results in graph-theoretic topology control and develop a joint power control and carrier sense threshold tuning algorithm that properly takes account of the SINR constraint and yet explores spatial reuse for maximizing the network capacity? The technical contributions of our paper are as follows.

- By adopting the "divide and conquer" methodology, we identify that the problem of jointly controlling the

transmit power and the carrier sense threshold can be divided into two sub-problems. The first sub-problem is to find, given the locations of nodes, an appropriate power assignment that maintains network connectivity while mitigating interference among nodes. This sub-problem exactly corresponds to conventional topology control, and hence we can leverage any existing topology control algorithm to solve this sub-problem. The second problem is to devise an efficient algorithm for tuning the carrier sense threshold so as to fully exploit spatial reuse while taking account of the SINR constraint. This two-phase, joint control framework enables us to eliminate the major deficiency of conventional topology control, i.e., failure to take account of the effect of SINR, and to further improve the network capacity.

- We derive a desirable operating condition for the carrier sense threshold. Conceptually, each node can increase its chance for transmission by increasing its carrier sense threshold as long as the SINR constraint is satisfied. A difficulty in realizing this idea is how each node knows whether or not increasing the carrier sense threshold will lead to the violation of the SINR constraint given that *the node distribution is unknown and each node tunes its transmit power and carrier sense threshold independently*. It may be possible to maintain a desirable level of SINR by exchanging information among nodes, i.e., the SINR information is fed back from a receiver to its corresponding sender. Then, each node increases/decreases its carrier sense threshold if the current SINR is larger/smaller than the target SINR value [8]. From the perspective of implementation, however, it is more efficient to devise a fully distributed algorithm without any information exchange. Our analysis indicates that, similar to several other physical/thermodynamic systems, there exists a phase transition (i.e., an abrupt increase in the collision probability) as the carrier sense threshold increases. As a result, each node can maximize its throughput by simply observing its transmission collision probability, without introducing any additional feedback mechanism.
- Based on our previous topology control work, *localized minimal spanning tree (LMST)* [3], we devise an exemplary algorithm, called *LMST with Dynamic Carrier Sense Adaptation (LMST-DCSA)*, to demonstrate the utility of the proposed joint control framework. In LMST-DCSA, each node first determines an appropriate power assignment with LMST and then adaptively tunes the carrier sense threshold to further improve the network performance. It should be noted that the proposed joint control framework is rather general and not restricted to LMST. By virtue of the insight shed from our analysis, we can devise a fully localized algorithm for tuning the carrier sense threshold, and consequently exploiting spatial reuse under the physical SINR model. As such, the joint control framework plays a crucial role of bridging the gap between graph-theoretic topology control and SINR-based control of PHY/MAC attributes in CSMA/CA wireless networks. Through simulation in J-Sim [9], we show the superiority of LMST-DCSA to LMST, thus demonstrating the utility and effectiveness of the proposed framework. Also, we show that the network performance with topology control alone can be even worse than that without topology control, if the carrier sense threshold is not appropriately chosen. This observation implies that *joint control* of transmit power and carrier sense threshold is crucial for improving the network performance.

The remainder of this paper is organized as follows. In Section II, we provide an overview of related work, and give the technical motivation of this work. In Section III, we give the model and related notions used in our analysis. In Section IV, we present a joint control framework for determining both the transmit power and the carrier sense threshold. In particular, we elaborate on the issue of tuning the carrier sense threshold of each node in a fully distributed manner, and devise LMST-DCSA as an exemplary joint control algorithm. Following that, we evaluate the performance of LMST-DCSA in Section V, and conclude the paper in Section VI with a list of future research avenues.

II. Related Work

A. Transmit Power Control

The issue of transmit power control has been extensively studied under the graph-theoretic model, where two nodes are considered neighbors and a wireless link exists between them, if their distance is within the transmission range (as determined by the transmit power, the path loss model, and the receiver sensitivity) of each other [2]–[6]. The main objective of graph-theoretic topology control is to preserve network connectivity with each node transmitting with the minimal possible power. For example, LMST [3] is a localized algorithm that guarantees network connectivity and provides a bound (of six) on the node degree. The interested reader is referred to [10] for a detailed taxonomy of conventional topology control algorithms.

Use of transmit power control for maximizing the network capacity under the physical SINR model has been considered in [11]–[13]. Monks *et al.* [11] proposed a power control protocol called PCMA, in which the receiver advertises its interference margin that it can tolerate on an out-of-band channel and the transmitter selects its power in order not to disrupt any ongoing transmissions. Muqattash and Krunz [12], [13] also proposed similar power control protocols called respectively PCDC and POWMAC. The PCDC protocol constructs the network topology by overhearing RTS/CTS packets, and the computed interference margin is announced on an out-of-band channel. The POWMAC protocol uses a single channel for exchanging the interference margin information.

As mentioned in Section I, the first category of graph-theoretic topology control does not take into account of the SINR constraint. The second category of power control algorithms, on the other hand, does not explicitly consider network

connectivity. Moreover, all the protocols do not consider the effect of the carrier sense threshold although it is a major determinant for spatial reuse.

B. Studies on Physical Carrier Sense for Improving Spatial Reuse

Recently, a number of studies have been carried out to study how physical carrier sense affects spatial reuse [8], [14]–[16]. In these studies, the carrier sense threshold was the main parameter for controlling the level of spatial reuse. Given a predetermined transmission rate, Zhu *et al.* [16] derived simple conditions for the carrier sense threshold in order to cover the entire interference range for several regular topologies. Zhu *et al.* also proposed in [8] a dynamic algorithm for adjusting the carrier sense threshold to exploit spatial reuse. Vasan *et al.* [15] proposed an algorithm, entitled *echos*, for on-line tuning of the carrier sense threshold in order to allow more flows in IEEE 802.11-based hotspot wireless networks. Nadeem *et al.* [14] proposed an enhanced DCF algorithm that exploits location information to exploit spatial reuse for given transmission rates.

There have also been a number of studies on the relation between physical carrier sense and Shannon capacity [17]–[20]. Yang and Vaidya [17] are perhaps the first to address the impact of physical carrier sense on Shannon capacity of wireless ad hoc networks, while taking account of the MAC layer overhead. Kim *et al.* [18] studied the relation between physical carrier sense and Shannon capacity, and showed that, in the case that the achievable channel rate follows the Shannon capacity, spatial reuse only depends on the ratio of the transmit power to the carrier sense threshold. Zhai and Fang [19] investigated the impact of physical carrier sense in multi-rate wireless networks where nodes have different levels of transmit power. Lin and Hou [20] studied the relation between the carrier sense threshold and the MAC throughput in multi-rate wireless networks, and identified that the MAC throughput has several transitional points caused by multiple data rates.

C. Joint Control of Transmit Power and Carrier Sense Threshold

The problem of jointly determining the transmit power and the carrier sense threshold has not been extensively studied in spite of its importance. Fuemmeler *et al.* [21] studied the relation between the transmit power and the carrier sense threshold, and showed that senders should keep the product of their transmit power and carrier sense threshold fixed at a constant. Yang *et al.* [22] proposed a joint control algorithm, called *LMST with Carrier Sense Adjustment (LMST-CSA)*, where the transmit power of a node is determined by LMST, and the carrier sense threshold is determined so as to eliminate all the hidden nodes. In spite of its simplicity, LMST-CSA requires channel information such as the path loss exponent for carrier sense threshold adjustment. Furthermore, it does not explicitly consider the SINR constraint, and thus may not fully exploit spatial reuse.

III. Interference and Node Throughput Models

In this section, we introduce the network model and notions used in our analysis. Then, we derive an analytical model of the saturation node throughput as a function of the carrier sense threshold.

A. Channel Propagation and Interference Model

Consider a wireless network consisting of a set of N nodes, denoted by $\mathcal{N} = \{1, \cdots, N\}$. For a given node $i \in \mathcal{N}$, let $r(i) \in \mathcal{N}$ denote the corresponding receiver. Let P_i denote the transmit power of node i, and θ the path loss exponent (which typically ranges between 2 and 4). Then the received power at $r(i)$ can be expressed as $P_{r(i)} = P_i / d_{i,r(i)}^{\theta}$, where $d_{i,j}$ denotes the distance between nodes i and j. As a necessary condition for the receiver $r(i)$ to correctly decode the symbols, $P_{r(i)}$ should be larger than or equal to the receive threshold of $r(i)$, denoted by $\gamma_{r(i)}$, i.e.,

$$P_{r(i)} = \frac{P_i}{d_{i,r(i)}^{\theta}} \geq \gamma_{r(i)}. \tag{1}$$

By (1), the transmission range $d_T(i, r(i))$, which is the maximum of $d_{i,r(i)}$ satisfying (1), can be obtained as $d_T(i, r(i)) = \left(P_i/\gamma_{r(i)}\right)^{\frac{1}{\theta}}$. In addition to (1), the received power $P_{r(i)}$ should be large enough so that the interference from other nodes does not prevent the receiver from correctly decoding the symbols. This condition can be expressed as

$$\text{SINR}_{r(i)} = \frac{P_{r(i)}}{I_{r(i)}} \geq \beta_{r(i)}. \tag{2}$$

Here, $I_{r(i)}$ is given as $I_{r(i)} = \sum_{j \neq i} P_j d_{j,r(i)}^{-\theta} + N_{r(i)}$ where $N_{r(i)}$ is the ambient noise, and $\beta_{r(i)}$ is called the SINR threshold of the receiver $r(i)$.

The *collision set* of receiver $r(i)$, denoted by $C_{r(i)}$, is defined as the set of nodes whose simultaneous transmission with node i will prevent $r(i)$ from correctly decoding the symbols of node i, i.e.,

$$C_{r(i)} = \left\{ j \middle| \frac{P_{r(i)}}{P_j d_{j,r(i)}^{-\theta}} < \beta_{r(i)} \right\} = \{ j | d_{j,r(i)} < d_C(i,j) \},$$

where $d_C(i,j) := \left(P_j \beta_{r(i)} / P_i\right)^{\frac{1}{\theta}} d_{i,r(i)}$.

Let x_i denote the carrier sense threshold of node i. If the signal strength perceived at node i is larger/smaller than x_i, the channel is considered busy/idle by node i. For a given node i, let $S_i(x_i)$ denote the *carrier sense set* of node i, which is defined as

$$S_i(x_i) = \left\{ j | P_j d_{i,j}^{-\theta} \geq x_i \right\} = \left\{ j | d_{i,j} \leq d_S(i,j) \right\},$$

where $d_S(i,j) := (P_j / x_i)^{\frac{1}{\theta}}$ is termed as the carrier sense range. Hence, node i will be silenced if any node in $S_i(x_i)$ transmits. In a similar manner, let L_i denote the *silence set* of node i, which is defined as

$$L_i = \left\{ j | P_i d_{i,j}^{-\theta} \geq x_j \right\} = \left\{ j | d_{i,j} \leq d_L(i,j) \right\},$$

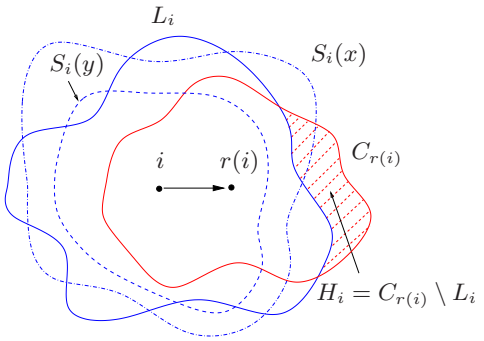

Fig. 1. Set relation among $C_{r(i)}$, L_i, H_i, $S_i(x)$, and $S_i(y)$ ($x < y$).

where $d_L(i,j) := (P_i/x_j)^{\frac{1}{\theta}}$ is termed as the silenced range. Thus, every node $j \in L_i$ will be silenced when node i transmits. Finally, let H_i denote the set of hidden nodes with respect to node i, which is defined as $H_i = C_{r(i)} \setminus L_i$. Thus, no node in H_i can detect the transmission of node i. Moreover, if any node in H_i transmits during the transmission of node i, the transmission of node i will fail. This is the well known hidden node problem.

For a given transmission from node i to node $r(i)$, Fig. 1 shows the relation between $C_{r(i)}$, L_i, H_i, and $S_i(x_i)$. By their definitions, the boundaries of $C_{r(i)}$, L_i, and $S_i(x_i)$ are determined by such as the node distribution, the power assignment, and the carrier sense thresholds. Hence, they can be arbitrary shapes in general. It should be noted that $C_{r(i)}$, L_i, and H_i are all independent of x_i by their definitions. Only $S_i(x_i)$ is a function of x_i, and satisfies $S_i(y) \subset S_i(x)$ if $x < y$ from its definition. As a matter of fact, what carrier sense of each node does is *not* to prevent other nodes from transmitting, *but* to detect (before each transmission attempt) the status of the channel in $S_i(x_i)$. Hence, even when $C_{r(i)} \subset S_i(x_i)$, node i's transmission may still fail if interrupted by a single transmission in H_i ($\subset C_{r(i)}$) or multiple transmissions in $(\mathcal{N} \setminus C_{r(i)}) \setminus L_i$.

B. Node Throughput in Multi-hop Wireless Networks

Now we derive the saturation node throughput as a function of the carrier sense threshold. Although the derivation is similar to those in [22]–[24], one major difference is that we explicitly take into account of the carrier sense threshold and the SINR constraint.

Let τ_i and v_i denote, respectively, the channel access probability that node i attempts to transmit in a virtual slot[1], and the average virtual slot time of node i. At any time instance, the channel status of node i will be in one of the following three states: *Busy*, *Idle*, and *Deferring*. In the *Busy* (*Idle*) state, node i is transmitting (idle). Note that we do not distinguish whether the transmission is successful or not in the *Busy* state. This is because both a collision and a transmission success take approximately the same amount of time, and much larger than that taken in the *Idle* state [22]. In the *Deferring* state, node i is being deferred due to other ongoing transmissions. Let t_B, t_I, and t_D denote the average duration of the *Busy*, *Idle*, and *Deferring* states, respectively. Also, let τ_{ji} denote the channel access probability of node j as perceived by node i, which is assumed to be independent and identically distributed among j. Now, the average virtual slot time v_i can be expressed as

$$\begin{aligned} v_i(x_i) =& \tau_i t_B + (1-\tau_i)\mathbb{E}\Big[\prod_{j\in S_i}(1-\tau_{ji})\Big] t_I + (1-\tau_i) \\ & \times \Big(1 - \mathbb{E}\Big[\prod_{j\in S_i}(1-\tau_{ji})\Big]\Big) t_D \\ =& \tau_i t_B + (1-\tau_i)\left[t_D - (t_D - t_I)(1-\overline{\tau}_{-i})^{|S_i(x_i)|}\right], \end{aligned} \tag{3}$$

where $\overline{\tau}_{-i} = \mathbb{E}[\tau_{ji}]$. Here, it is assumed that t_B, t_I, t_D, τ_{ji}'s, and thus $\overline{\tau}_{-i}$ are independent of x_i.

There are two sources of transmission collisions, i.e., collision incurred by simultaneous transmissions in $C_{r(i)}$ and collision incurred by multiple transmissions outside $C_{r(i)}$ that causes the SINR constraint to be violated at node $r(i)$. Let $q_i(x_i)$ denote the conditional collision probability of node i given that a transmission attempt is made. Then, we have

$$\begin{aligned} q_i(x_i) =& P[\text{Transmission in } C_{r(i)}] + P[\text{No transmission in } C_{r(i)}] \\ & \times P[\text{SINR}_{r(i)} < \beta_{r(i)} | \text{No transmission in } C_{r(i)}] \\ =& p_i + (1-p_i)h_i(x_i), \end{aligned} \tag{4}$$

where $p_i := P[\text{Transmission in } C_{r(i)}]$ and $h_i(x_i) := P\left[\text{SINR}_{r(i)} < \beta_{r(i)} | \text{No transmission in } C_{r(i)}\right]$.

To derive p_i, we consider the event of no transmission in $C_{r(i)}$. This event occurs when (i) all the nodes in $C_{r(i)}$ do not simultaneously transmit with node i *and* (ii) all the hidden nodes in $C_{r(i)} \setminus L_i$ do not transmit *during the vulnerable period* V. Here, V is the interval during which the transmission from node i to node $r(i)$ will fail if any node in H_i attempts to transmit. V can be expressed as $V = T_H + T_P$, where T_H and T_P are, respectively, the time required to transmit the header and the payload. Now, p_i can be expressed as

$$p_i = 1 - (1-\overline{\tau}_{-i})^{|C_{r(i)}|}(1-\overline{\tau}_{-i})^{\sum_{k\in H_i}\frac{V}{v_k}}. \tag{5}$$

Here, note that p_i in (5) is not a function of x_i, but a function of x_j's, $j \in C_{r(i)}$.

It is much more difficult to derive $h_i(x_i)$, because $h_i(x_i)$ depends primarily on the probability distribution of accumulative interference that results from *concurrent* transmissions *outside* the collision set. This probability distribution, in turn, depends on the spatial distribution of sender/receiver pairs and their traffic patterns, and is not available in general. Hence, instead of directly deriving $h_i(x_i)$, we will derive a general property of $h_i(x_i)$ in Proposition 2 in Section IV-B.

By (3) and (4), we can readily obtain the throughput of node i as

$$T_i(x_i) = \frac{L\tau_i\big(1-q_i(x_i)\big)}{v_i(x_i)} = U_i(x_i)(1-q_i(x_i)), \tag{6}$$

[1]Following Bianchi's notion [25], we define a virtual slot as the interval between two consecutive events.

where $U_i(x_i) = L\tau_i/v_i(x_i)$ and L is the payload size. Note that $U_i(x_i)$ corresponds to the sending rate of node i, and $1 - q_i(x_i)$ is the probability of successful transmissions. Note also that T_i is a function of not only x_i (as explicitly shown in (6)), but also P_i, P_j's, and x_j's, because P_i, P_j's, and x_j's are implied in the definition of $C_{r(i)}$, L_i, H_i, and $S_i(x_i)$.

IV. Joint Control Framework

In this section, we present a joint control framework for determining the transmit power and the carrier sense threshold. To demonstrate the utility of the framework, we also devise a joint power control and carrier sense tuning algorithm, called LMST-DCSA.

A. Separation between Transmit Power Control and Carrier Sense Adaptation

Given the locations of nodes, we first consider the most general problem of joint controlling the transmit power and the carrier sense threshold, with the objective of maximizing the overall system throughput, subject to a network connectivity constraint. The problem can be formulated as

$$\text{maximize} \left[T(\mathbf{x}, \mathbf{P}) = \sum_{i=1}^{N} T_i(\mathbf{x}, \mathbf{P}) \right] \quad \text{(P1)}$$
$$\text{subject to a connectivity constraint on } \mathbf{P},$$

where $\mathbf{x} = (x_1, \cdots, x_N)$, $\mathbf{P} = (P_1, \cdots, P_N)$, and $x_i \in [x_{\min}, x_{\max}]$, $P_i \in [P_{\min}, P_{\max}]$, $i = 1, \cdots, N$. It is a formidable task to find an optimal solution to (P1) for several reasons. First, (P1) is highly nonlinear in that there exists interdependency among $\mathbf{x}$ and $\mathbf{P}$ because $T(\mathbf{x}, \mathbf{P})$ depends on x_i/P_j, $i, j \in \mathcal{N}$. Thus, it is extremely difficult to find a global optimal solution to (P1). Furthermore, a connectivity constraint on $\mathbf{P}$ may result in a very complex feasible region.[2]

Instead of attempting to find an optimal solution to (P1), we introduce a two-phase, joint control framework which provides a sub-optimal solution to (P1). The key idea is to consider $\mathbf{P}$ and $\mathbf{x}$ separately based on the observation that network connectivity depends only on $\mathbf{P}$. First, we determine $\mathbf{P}$, with the objective of preserving network connectivity while mitigating MAC-level interference. This problem exactly corresponds to that of conventional topology control, and we can readily leverage an existing topology control algorithm for solving the first problem. Once we obtain a power assignment $\mathbf{P}$, we then tune $\mathbf{x}$, and improve the throughput sustained by each node, while properly taking account of the SINR constraint. Through this two-step framework, we can leverage existing results in graph-theoretic topology control, and further improve the network performance by tuning the carrier sense threshold.

[2]In fact, the problem of finding an optimal power assignment $\mathbf{P}$ with fixed values of $\mathbf{x}$ and with the objective of minimizing the energy cost in graph-theoretic topology control has been shown to be NP hard [10].

B. Desirable Operating Condition for Carrier Sense Threshold

Given that we will leverage an existing topology control algorithm for determining the transmit power, what remains is to determine an appropriate value of the carrier sense threshold for each node, so as to fully exploit spatial reuse subject to the SINR constraint. Conceptually, each node i needs to increase its carrier sense threshold as much as possible, in order to maximize its chance for transmission. On the other hand, the larger the carrier sense threshold, the lower the SINR that can potentially be sustained at the receiver. This is because the number of nodes in $S_i(x_i)$ decreases as x_i increases, which, in turn, leads to larger accumulative interference that results from concurrent transmissions outside $S_i(x_i)$. Thus, x_i should be appropriately set to balance out these two conflicting factors.

To analytically validate the above reasoning, we first show the following property of $U_i(x_i)$ in (6).

Proposition 1 *$U_i(x_i) = L\tau_i/v_i(x_i)$ in (6), which is the sending rate of node i, increases in x_i.*

Proof: By (3), we have

$$\frac{\partial v_i}{\partial x_i} = K \frac{d|S_i|}{dx_i}, \quad (7)$$

where $K = -\log(1 - \overline{\tau}_{-i})(1 - \tau_i)(t_D - t_I)(1 - \overline{\tau}_{-i})^{|S_i|}$. Given any reasonable CSMA/CA protocol, e.g., IEEE 802.11 protocol, $K > 0$ because $t_D \gg t_I$ [22]. Furthermore, for all x, y with $x < y$,

$$S_i(y) = \{j | P_j d_{i,j}^{-\theta} \geq y\} \subset \{j | P_j d_{i,j}^{-\theta} \geq x\} = S_i(x).$$

Thus, $|S_i(x)| \geq |S_i(y)|$ for all x, y with $x < y$, or equivalently $d|S_i(x_i)|/dx_i \leq 0$. By plugging this result into (7), we have $dv_i/dx_i \leq 0$. Consequently,

$$\frac{\partial U_i}{\partial x_i} = -\frac{L\tau_i}{v_i^2} \frac{\partial v_i}{\partial x_i} \geq 0,$$

because L and τ_i are obviously independent of x_i, and p_i in (5) is independent of x_i because $C_{r(i)}$, H_i, $\overline{\tau}_{-i}$, and v_k where $k \in H_i$ are all independent of x_i by their definitions. ■

Second, we show $h_i(x_i)$ in (4) — the probability that the SINR constraint is not satisfied given no transmission in $C_{r(i)}$ — has the following property.

Proposition 2 *$h_i(x_i)$ in (4) increases in x_i.*

Proof: We express the interference $I_{r(i)}$ in (2) with two terms, i.e., $I_{r(i)} = I_{r(i)}^c + I_{r(i)}^a(x_i)$, where $I_{r(i)}^c = \sum_{j \in C_{r(i)}} P_j d_{j,r(i)}^{-\theta}$ and $I_{r(i)}^a(x_i) = \sum_{j \neq i, j \in \mathcal{N} \setminus C_{r(i)}} P_j d_{j,r(i)}^{-\theta} + N_{r(i)}$. Note that $I_{r(i)}^c$ is independent of x_i by the definition of $C_{r(i)}$. Now, $h_i(x_i)$ in (4) is expressed as

$$\begin{aligned} h_i(x_i) =& P\left[\text{SINR}_{r(i)} < \beta_{r(i)} | \text{No transmission in } C_{r(i)}\right] \\ =& P\left[\frac{P_{r(i)}}{I_{r(i)}^c + I_{r(i)}^a(x_i)} < \beta_{r(i)} \middle| I_{r(i)}^c = 0\right] \\ =& P\left[I_{r(i)}^a(x_i) > \frac{P_{r(i)}}{\beta_{r(i)}}\right]. \end{aligned} \quad (8)$$

Here, $I^a_{r(i)}(x_i)$ is contributed by two sources. The first source is the interference from concurrent transmissions of nodes in $(\mathcal{N} \setminus C_{r(i)}) \setminus L_i$, which does not sense the transmission of node i and begins during the interval when node i transmits. The second source results from transmissions in $(\mathcal{N} \setminus C_{r(i)}) \setminus S_i(x_i)$, which have already been ongoing but cannot be detected by node i when node i starts transmission. Since $S_i(y) \subset S_i(x)$ for all x, y with $x < y$, from the proof in Proposition 1, we have $(\mathcal{N}\setminus C_{r(i)})\setminus S_i(x) \subset (\mathcal{N}\setminus C_{r(i)})\setminus S_i(y)$ if $x < y$, which gives $I^a_{r(i)}(x) \preceq I^a_{r(i)}(y)$ for all x, y with $x < y$. Consequently, we have $h_i(x) \leq h_i(y)$ for all x, y with $x < y$. ■

Third, we show that the collision probability $q_i(x_i)$ in (4) has the following property.

Proposition 3 *$q_i(x_i) = p_i + (1 - p_i)h_i(x_i)$ in (4) increases in x_i.*

Proof: By (5) together with the fact that $C_{r(i)}$, H_i, $\overline{\tau}_{-i}$, and v_k, $k \in H_i$ are all independent of x_i by their definitions, p_i is independent of x_i. Thus, by (4) and Proposition 2, we have $\partial q_i/\partial x_i = (1 - p_i)\partial h_i/\partial x_i \geq 0$. ■

By (8), only when the distribution of $I^a_{r(i)}(x_i)$ is given, one can obtain an explicit form of $h_i(x_i)$. However, since $\mathbb{E}[I^a_{r(i)}(x_i)]$ decreases in x_i (from $I^a_{r(i)}(x) \preceq I^a_{r(i)}(y)$, $x < y$), we can infer that there generally exists a critical value of x_i, denoted by x^c_i, around which $h_i(x_i)$ will abruptly change (probably $\mathbb{E}[I^a_{r(i)}(x^c_i)] \simeq P_{r(i)}/\beta_{r(i)}$.) Since p_i is independent of x_i, $q_i(x_i)$ will exhibit a sudden increase around x^c_i as a result of the abrupt change in $h_i(x_i)$. With this insight and Propositions 1 and 3, we can depict the relation between $T_i(x_i)$, $U_i(x_i)$, $q_i(x_i)$, and x^c_i in Fig. 2. As shown in Fig. 2, x_i should be kept around x^c_i in order to fully exploit spatial reuse and maximize $T_i(x_i)$ while properly satisfying the SINR requirement. Hence, a desirable operating point of x_i can be reached by increasing x_i *as long as* $q_i(x_i)$ *is maintained below a reasonable threshold*. (The relation depicted in Fig. 2 will be corroborated via simulation in Section V.) We will leverage this important observation in the joint control framework, and devise an exemplary algorithm which adjusts x_i towards x^c_i.

One point is worthy of mentioning. From Fig. 2, it may seem plausible to observe T_i, rather than q_i, and control x_i accordingly. However, note that T_i is a function of *not only* node i's own carrier sense threshold x_i, *but also* other nodes' carrier sense thresholds x_j's. Given that each node independently tunes its carrier sense threshold, the change in T_i may come from that in other nodes' carrier sense thresholds, and does not necessarily reflect the current SINR level. Consequently, in order to properly take into account of the effect of SINR on the node throughput, it is more appropriate to observe the collision probability q_i.

C. Joint Control Algorithm for Determining Transmit Power and Carrier Sense Threshold

We give an exemplary, joint control algorithm for determining the transmit power and carrier sense threshold to demonstrate the utility of the proposed joint control framework. Without loss of generality, we use a localized topology control algorithm, LMST, as the component algorithm for power control. For the completeness of the paper, we briefly summarize LMST. The interested reader is referred to [3] for a detailed account of LMST and its properties.

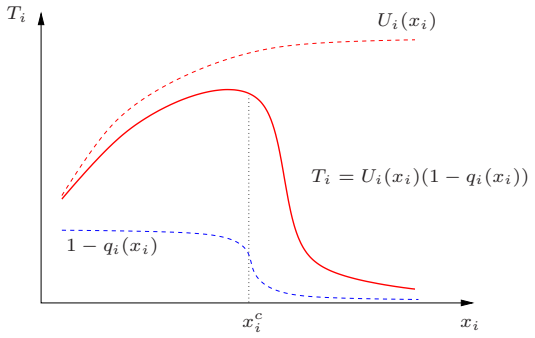

Fig. 2. Throughput of node i as a function of its carrier sense threshold given that the carrier sense thresholds of all the other nodes are fixed.

1) Transmit Power Control by LMST: LMST is composed of three phases: *information collection*, *topology construction*, and *determination of transmit power*. In the information collection phase, the information needed by each node for topology construction is obtained by having each node periodically broadcast a Hello message using its maximal transmit power. A Hello message includes the node id and the position of the node. In this manner, each node knows which other nodes are in its neighborhood and their positions. In the topology construction phase, each node independently applies Prim's algorithm [26] to obtain its local minimum spanning tree in the neighborhood. In the power determination phase, each node takes only the one-hop, on-tree nodes as its neighbors, and determines the minimal power needed to reach all its neighbors.

2) Dynamic Carrier Sense Adaptation (DCSA): Now given the power assignment by LMST, we discuss how to dynamically control the carrier sense threshold of node i, based on the insight shed from our analysis in Section IV-B. As shown in Algorithm 1, for each time interval of T, node i calculates its collision probability q_i as $q_i = N_c/N_t$, where N_c and N_t are, respectively, the total number of collisions and the total number of transmission attempts made in the interval. Then, node i updates its carrier sense threshold x_i as follows: If q_i is larger than $(1+w)q_{\text{th}}$ where q_{th} is a given threshold and w is a weighting factor with $0 < w < 1$, then x_i is decremented by δ. Otherwise, if q_i is smaller than $(1 - w)q_{\text{th}}$, then x_i is incremented by δ.

There are several tunable parameters in Algorithm 1, i.e., q_{th}, T, δ, and w, whose values need to be determined. Fortunately, the network performance is quite robust to the choice of these parameters (provided that they are chosen within reasonable regions) for the following reasons. In principle, T, δ, and w are mainly related to how fast the algorithm converges and are not critical to the throughput performance. Specifically, the larger the value of T, the slower the convergence speed.

Algorithm 1 Carrier sense adaptation of node i

```
Reset timer t
N_t ← 0 and N_c ← 0
while t < T do
    if node i transmits then
        N_t ← N_t + 1
        if transmission fails then
            N_c ← N_c + 1
        end if
    end if
end while
q_i ← N_c/N_t
if q_i > (1 + w)q_th then
    x_i ← x_i − δ
else
    if q_i < (1 − w)q_th then
        x_i ← x_i + δ
    end if
end if
```

As long as T is large enough to properly estimate the collision probability q_i, the network performance will not change significantly for different values of T. (In the simulation study, the value of T is chosen in the range of several seconds.) The step size δ is also related to the convergence speed. The larger the value of δ, the faster the algorithm drives towards the equilibrium. Meanwhile, the algorithm may not converge but instead oscillate around the equilibrium point when δ is set to an inappropriately large value. Because the speed at which the algorithm converges is not our major concern, we set δ to a small value. A weighting factor w is introduced to prevent the algorithm from unnecessary oscillation and to make x_i remain in $[\underline{x}_i, \overline{x}_i]$ where $\underline{x}_i = q_i^{-1}((1-w)q_{\rm th})$ and $\overline{x}_i = q_i^{-1}((1+w)q_{\rm th})$. In principle, w needs to be proportional to δ, and with a small value of δ, w does not affect the performance significantly unless it is set to an unreasonably small value.

The most critical parameter is the collision probability threshold $q_{\rm th}$. If $q_{\rm th}$ is set to an inappropriately large value, the network performance will degrade due to excessive transmission collisions. On the other hand, if $q_{\rm th}$ is set to an inappropriately small value, the carrier sense threshold x_i will become unnecessarily small and the network performance will degrade as a result of insufficient spatial reuse. As mentioned in Section IV-B, there is an abrupt increase in q_i as x_i increases. This implies that the network performance will be quite insensitive to $q_{\rm th}$ unless $q_{\rm th}$ is so small that x_i converges to an unreasonably small value with Algorithm 1. We will further elaborate on the effect of $q_{\rm th}$ via simulation in the next section.

V. Simulation Studies

In this section, we evaluate the performance of LMST-DCSA with LMST and basic CSMA/CA (no-LMST) via simulation with J-Sim [9]. We use IEEE 802.11a as the PHY/MAC protocol. The default values of parameters used in the simulation are given in Table I. In particular, to precisely quantify the impact of carrier sense adaptation on the throughput performance, we disable the binary exponential back-off (BEB) mechanism and use a fixed contention window size of 63 as given in Table I. (Note that even when BEB is enabled, our simulation studies showed that LMST-DCSA still significantly outperforms LMST and no-LMST, which are omitted due to the page limit.) A total of N nodes are randomly distributed in an area of 500×500 m^2. Half of the nodes are randomly selected as sources and for each source, a receiver is randomly selected from its one-hop neighbors. The two-ray ground model is used as the propagation model. For LMST and LMST-DCSA, the transmit power used by each node is determined by LMST in Section IV-C1 while for no-LMST, all nodes use the same transmit power that gives a transmission range of 100 m. All sources generate CBR traffic at their full data rate. For LMST-DCSA, every node sets the initial value of its carrier sense threshold to -85 dBm.

TABLE I
Parameters used in the simulation studies.

Parameter	Value	Definition
N	100	Number of nodes
L	1024 bytes	Payload size
R	6, 18, 36, 54 Mbps	Data rate
CW	63	Fixed contention window size
$d_{\rm max}$	100 m	Maximal transmission range
$q_{\rm th}$	0.2	Collision probability threshold
w	0.1	Weighting factor
δ	0.5 dBm	Update step size
T	5 seconds	Update interval

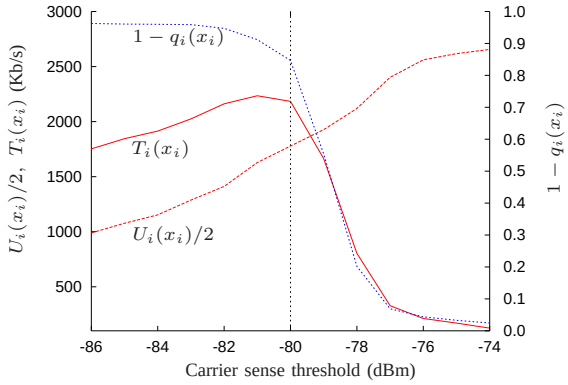

Fig. 3. Node throughput vs. carrier sense threshold (simulation result of Fig. 2).

Validation of Phase Transition: To validate the crucial observation made in Fig. 2, we carry out simulation with $R = 18$ Mb/s and LMST as the topology control algorithm. Figure 3 depicts the node throughput $T_i(x_i)$, the sending rate $U_i(x_i)$, and the probability of successful transmission $1 - q_i(x_i)$ versus the carrier sense threshold x_i. (Note that for the purpose of displaying both $T_i(x_i)$ and $U_i(x_i)$ in the same figure, we plot $U_i(x_i)/2$ instead of $U_i(x_i)$ in Fig. 3.) As expected, simulation results in Fig. 3 matches analytical results in Fig. 2 quite well, and the phase transition phenomenon is corroborated in the simulation. If the carrier sense threshold exceeds a certain threshold, e.g., -80 dBm, the probability of successful transmission sharply decreases, leading to an abrupt

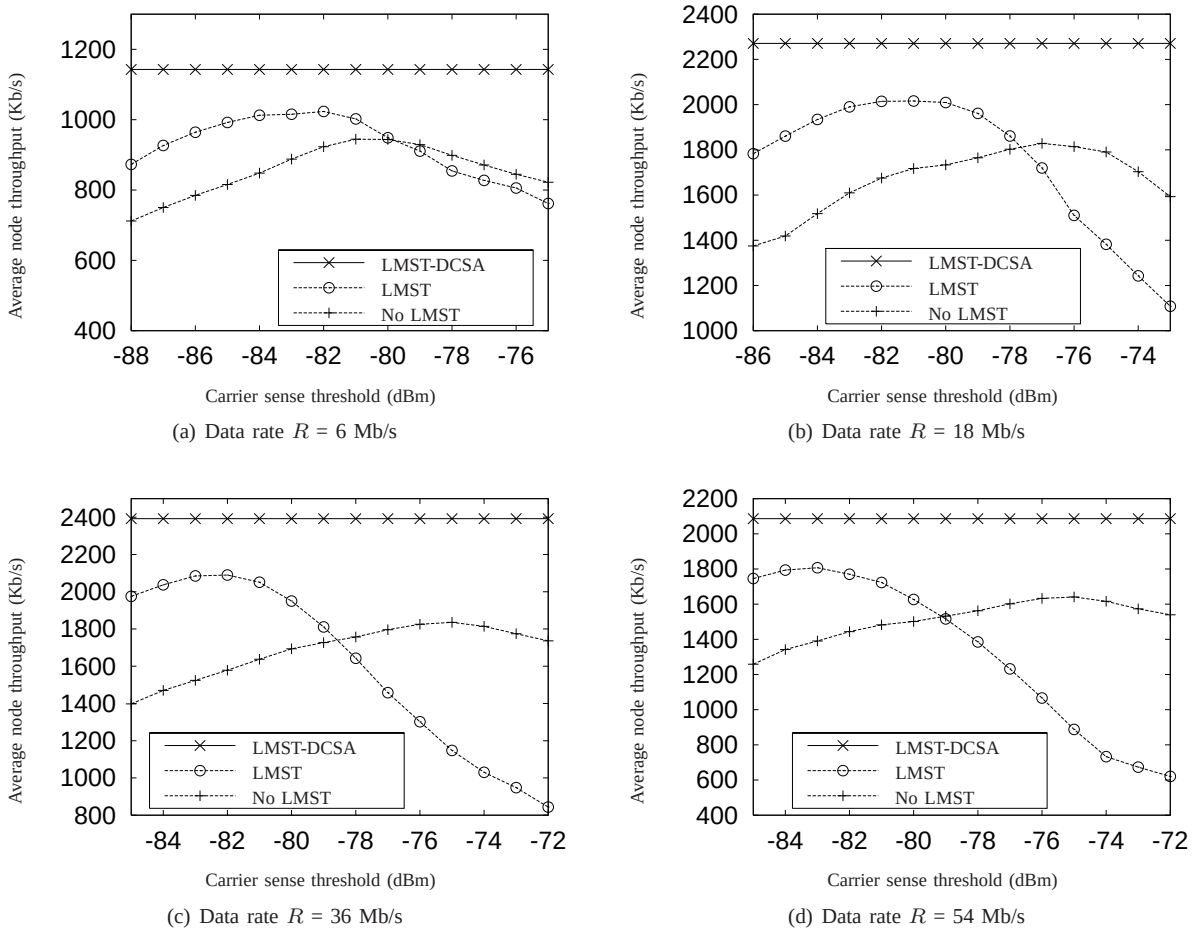

(a) Data rate R = 6 Mb/s

(b) Data rate R = 18 Mb/s

(c) Data rate R = 36 Mb/s

(d) Data rate R = 54 Mb/s

Fig. 4. Average node throughput versus carrier sense threshold.

degradation in the node throughput.

Performance Comparison: Figure 4 gives the average per-node throughput (averaged over all the nodes) versus the carrier sense threshold for different values of $R = 6$, 18, 36 and 54 Mb/s, respectively. Note that the x-axis in Fig. 4 does not apply to LMST-DCSA, because it exercises a dynamic control algorithm for tuning the carrier sense threshold. As shown in From Fig. 4, LMST-DCSA achieves much better throughput performance than LMST as well as no-LMST at all data rates. Specifically, LMST-DCSA achieves 21.01%, 24.19%, 30.32%, and 27.15% higher throughput than the maximal throughput achieved by no-LMST at $R = 6$, 18, 36, and 54 Mb/s, respectively; and 11.69%, 12.63%, 14.48%, and 15.44% higher throughput than the maximal throughput achieved by LMST at $R = 6$, 18, 36, and 54 Mb/s, respectively. In practice, it is extremely difficult to set an optimal carrier sense threshold under both LMST and no-LMST. As shown in Fig. 4, if an inappropriate carrier sense threshold is chosen, both LMST and no-LMST give inferior throughput performance. This implies the performance of LMST-DCSA will be much better than that of LMST and no-LMST in practice.

We can also observe from Fig. 4 that the throughput achieved by LMST rapidly degrades and even becomes smaller than that with no-LMST, as the carrier sense threshold increases beyond the value that achieves the maximal throughput. This is because the number of transmission failures caused by the violation of the SINR constraint significantly increases as the carrier sense threshold increases. Since under LMST each node uses the minimal possible transmit power subject to network connectivity, the SINR perceived at a receiver can even be smaller than that under no-LMST. This, coupled with the fact that the interference becomes severe given a large carrier sense threshold, leads to the performance degradation. This observation also implies that *joint control* of transmit power and carrier sense threshold is crucial for improving the network performance. Furthermore, an algorithm that sets the carrier sense threshold to a fixed value will be insufficient since the optimal carrier sense threshold depends on various factors such as power assignment, carrier sense thresholds of other nodes, node distribution, and their traffic patterns. Therefore DCSA is very promising in that it is self-adaptive and operates in a fully distributed manner.

Effect of the collision probability threshold: We now investigate the effect of the collision probability threshold $q_{\rm th}$ on the throughput performance of LMST-DCSA. Figure 5

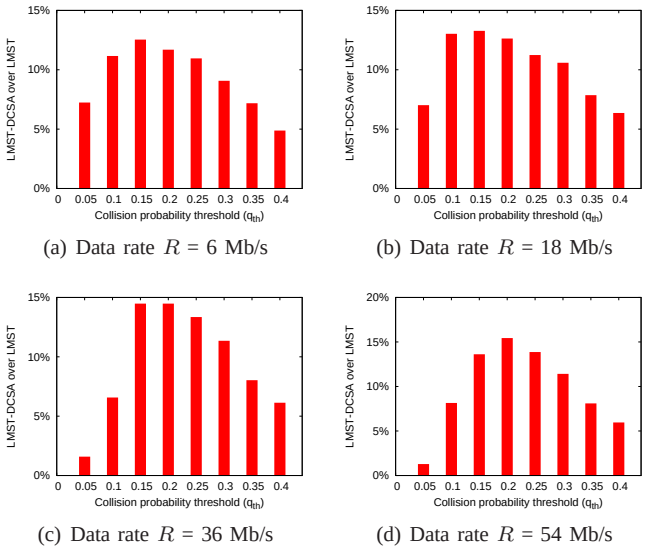

(a) Data rate R = 6 Mb/s (b) Data rate R = 18 Mb/s

(c) Data rate R = 36 Mb/s (d) Data rate R = 54 Mb/s

Fig. 5. Relative throughput gain of LMST-DCSA over LMST vs. collision probability threshold $q_{\rm th}$.

gives the relative throughput gain of LMST-DCSA over LMST versus $q_{\rm th}$ at $R = 6, 18, 36$, and 54 Mb/s. As shown in Fig. 5, the throughput performance of LMST-DCSA is not so much sensitive to $q_{\rm th}$ at all data rates as long as $q_{\rm th}$ lies in a reasonable region, e.g., $q_{\rm th} \in [0.15, 0.25]$.

VI. Conclusion

We have presented a joint control framework for determining the transmit power and the carrier sense threshold. The framework decouples the problem of jointly controlling the transmit power and the carrier sense threshold into two sub-problems. For the first power control sub-problem, we can leverage any existing localized topology control algorithm. To devise an efficient solution algorithm to the second sub-problem, we analyze a desirable operating condition for the carrier sense threshold, and show that there exists a phase transition (i.e., an abrupt increase in the collision probability) as the carrier sense threshold increases. By leveraging the insight shed from the analysis, we devise a simple algorithm to dynamically control the carrier sense threshold, so as to fully exploit spatial reuse while taking into account the SINR constraint. The major contribution of our work is that it bridges the gap between conventional graph-theoretic topology control and SINR-based control of PHY/MAC attributes in CSMA/CA wireless networks.

We are currently investigating several issues. In particular, the contention resolution mechanism such as the BEB mechanism in IEEE 802.11 is also influenced by the carrier sense threshold. Investigating the interaction between the proposed framework and the contention resolution mechanism will lead to performance improvement along another dimension.

References

[1] J. C. Hou, K.-J. Park, T.-S. Kim, and L.-C. Kung, "Medium access control and routing protocols for wireless mesh network," in *Wireless Mesh Networks: Architectures, Protocols, and Applications*, E. Hossain and K. K. Leung, Eds. Springer, 2007.

[2] N. Li and J. C. Hou, "Topology control in heterogeneous wireless networks: problems and solutions," in *Proc. of IEEE INFOCOM*, March 7–11 2004.

[3] N. Li, J. C. Hou, and L. Sha, "Design and analysis of a MST-based distributed topology control algorithm for wireless ad-hoc networks," *IEEE Trans. on Wireless Communications*, vol. 4, no. 3, pp. 1195–1207, 2005.

[4] R. Ramanathan and R. Rosales-Hain, "Topology control of multihop wireless networks using transmit power adjustment," in *Proc. of IEEE INFOCOM*, March 26–30 2000.

[5] V. Rodoplu and T. Meng, "Minimum energy mobile wireless networks," *IEEE Journal on Selected Areas in Communications*, vol. 17, no. 8, pp. 1333 – 1344, 1999.

[6] R. Wattenhofer, L. Li, P. Bahl, and Y.-M. Wang, "Distributed topology control for power efficient operation in multihop wireless ad hoc networks," in *Proc. of IEEE INFOCOM*, April 22–26 2001.

[7] T. Moscibroda, R. Wattenhofer, and A. Zollinger, "Topology control meets SINR: the scheduling complexity of arbitrary topologies," in *Proc. of ACM MobiHoc*, May 22–25 2006.

[8] J. Zhu, X. Guo, L. Yang, W. S. Conner, S. Roy, and M. M. Hazra, "Adapting physical carrier sensing to maximize spatial reuse in 802.11 mesh networks," *Wiley Wireless Communications and Mobile Computing*, vol. 4, pp. 933–946, December 2004.

[9] "J-Sim," http://www.j-sim.org/.

[10] P. Santi, "Topology control in wireless ad hoc and sensor networks," *ACM Computing Surveys*, vol. 37, no. 2, pp. 164–194, June 2005.

[11] J. Monks, V. Bharghavan, and W.-M. Hwu, "A power controlled multiple access protocol for wireless packet networks," in *Proc. of IEEE INFOCOM*, April 22–26 2001.

[12] A. Muqattash and M. Krunz, "Power controlled dual channel (PCDC) medium access protocol for wireless ad hoc networks," in *Proc. of IEEE INFOCOM*, March 30–April 3 2003.

[13] ——, "A single-channel solution for transmission power control in wireless ad hoc networks," in *Proc. of ACM MobiHoc*, May 24–26 2004.

[14] T. Nadeem, L. Ji, A. Agrawala, and J. Agre, "Location enhancement to IEEE 802.11 DCF," in *Proc. of IEEE INFOCOM*, March 13–17 2005.

[15] A. Vasan, R. Ramjee, and T. Woo, "ECHOS: enhanced capacity 802.11 hotspots," in *Proc. of IEEE INFOCOM*, March 13–17 2005.

[16] J. Zhu, X. Guo, L. Yang, and W. S. Conner, "Leveraging spatial reuse in 802.11 mesh networks with enhanced physical carrier sensing," in *Proc. of IEEE ICC*, June 20–24 2004.

[17] X. Yang and N. H. Vaidya, "On the physical carrier sense in wireless ad hoc networks," in *Proc. of IEEE INFOCOM*, March 13–17 2005.

[18] T.-S. Kim, H. Lim, and J. C. Hou, "Improving spatial reuse through tuning transmit power, carrier sense threshold, and data rate in multihop wireless networks," in *Proc. of ACM MobiCom*, September 24–29 2006.

[19] H. Zhai and Y. Fang, "Physical carrier sensing and spatial reuse in multirate and multihop wireless ad hoc networks," in *Proc. of IEEE INFOCOM*, April 23–29 2006.

[20] T.-Y. Lin and J. C. Hou, "Interplay of spatial reuse and SINR-determined data rates in CSMA/CA-based, multi-hop, multi-rate wireless networks," in *Proc. of IEEE INFOCOM*, May 6–12 2007.

[21] J. A. Fuemmeler, N. H. Vaidya, and V. V. Veeravalli, "Selecting transmit powers and carrier sense thresholds for CSMA protocols," Department of Electrical and Computer Engineering, University of Illinois at Urbana-Champaign, Tech. Rep., October 2004.

[22] Y. Yang, J. C. Hou, and L.-C. Kung, "Modeling of physical carrier sense in multi-hop wireless networks and its use in joint power control and carrier sense adjustment," in *Proc. of IEEE INFOCOM Miniconferences*, May 6–12 2007.

[23] M. Garetto, T. Salonidis, and E. W. Knightly, "Modeling per-flow throughput and capturing starvation in CSMA/CA multi-hop wireless networks," in *Proc. of IEEE INFOCOM*, April 23–29 2006.

[24] K. Duffy, D. J. Leith, T. Li, and D. Malone, "Modeling 802.11 mesh networks," *IEEE Communications Letters*, vol. 10, no. 8, pp. 635–637, August 2006.

[25] G. Bianchi, "Performance analysis of the IEEE 802.11 distributed coordination function," *IEEE Journal on Selected Areas in Comm.*, vol. 18, no. 3, 2000.

[26] R. Prim, "Shortest connection networks and some generalizations," *The Bell System Technical Journal*, vol. 36, pp. 1389–1401, 1957.